

RESEARCH

Open Access



# Development of a test method for the dynamic drapability of fabrics using reciprocating motion

Eunbi Yun<sup>1</sup> and Changsang Yun<sup>1\*</sup> 

\*Correspondence:  
cyun@ewha.ac.kr

<sup>1</sup> Department of Fashion Industry, Ewha Womans University, Ewhayeodae-Gil 52, Seodaemun-Gu, Seoul 03760, Republic of Korea

## Abstract

This study aimed to develop a method for measuring the dynamic drapability of fabrics using a reciprocating motion device that mimics the movement created by shaking a piece of fabric. Five types of fabrics were selected based on their drape coefficients and weights, and the lengths of fabrics were determined based on skirt length (50 cm) and dress length (100 cm). The width and speed of the reciprocating motion were considered as the experimental variables. Results of reciprocating motion-based fabric movement analysis revealed that the number of nodes, the position of the first node, amplitude, total length, and area are significant factors for measuring dynamic drapability. It was found that the longer fabrics had more nodes, enabling measurement of various types of fabrics. Furthermore, it was found that a wider reciprocation width under the same speed and a faster reciprocation speed with the same width favorably demonstrated dynamic drapability, resulting in proportionality between the reciprocating motion and the force transmitted to the fabric. Movement analysis of seven selected conditions and additional samples showed that the optimal condition was a 100-mm reciprocation width and a 150-rpm speed and that the first node's position is the most significant factor for a dynamic drapability. To verify the proposed measurement method, measuring four pairs of fabrics with similar drape coefficients but different shapes showed that as fabric weight increased, the node moved downward, despite similar drape coefficient values. This confirms that the proposed method can overcome the limitations of the existing drape coefficient.

**Keywords:** Drapability, Drape coefficient, Reciprocating motion, Fabric movement, Node position

## Introduction

The fashion industry has incorporated three-dimensional virtualization into clothing production and consumption, and virtual fitting technology has enabled checking the fit of apparel in virtual reality (Lim et al., 2009; Sarakatsanos et al., 2021). Such progress requires infrastructural technology that can minimize the differences between actual and virtual materials to facilitate the widespread utilization of virtual clothing.

Fabric drapability is a decisive factor in the silhouette of clothing (British Kenkare & May-Plumlee, 2005; Mooroka & Niwa, 1976; Standard, 1973), and is based on complex interaction between physical properties such as tensile, bending, and shear behaviors. Additionally, the bending stiffness, compressibility, surface friction, weight, wrinkle recovery, and thickness should be considered (Collier et al., 1989, 1991; Mooroka & Niwa, 1976; Süle, 2012).

Fabric drapability can be measured using static or dynamic methods. A common method is the static drape measurement method by G. E. Cusick's (1965), which calculates drapability by securing a circular fabric at the center between two smaller disks and measuring the area of the fabric naturally draping (British Standard, 1973). This method is useful because it can measure numerous fabrics' drapability in a short period of time, but it is often inadequate for describing actual clothes' drape shape (Kilic et al., 2021). Moreover, since the static drape coefficient is measured from a fixed position, it cannot reflect clothes' movement, triggering various studies on measuring dynamic drapability (Matsudaira et al., 2002).

To overcome the limitation of static drape measurements, Matsudaira et al. (2002) developed the dynamic drape coefficient with swing motion. To replicate dynamic drape behavior, G. B. Kilic proposed determining the rotating speed of a dynamic drape testing device by calculating the average walking speed of individuals. Through the correlations between mediating variables such as bending stiffness, shear deformation, and drape coefficient, Kilic et al. (2021) aimed to understand their relationship to fabric drape behavior. Wang and Cheng (2011) developed a dynamic drape testing device with a support disk fixture based on the swing speed and angle of the human body when walking and proposed a measuring method entailing different reciprocation speeds and angles. Ji et al. (2006) examined the dynamic drapability of fabrics by simulating a windy situation. The aforementioned studies attempted to measure dynamic drapability by transforming existing static drape testing devices using rotation, with the limitation that the conditions differ from actual fabrics comprising real clothes. For instance, clothes produced from real fabrics show back-and-forth swinging movements when people walk. Furthermore, during the process of selecting material for clothes at manufacturing sites, fabrics are held at each end and shaken to verify their drapability. Therefore, there is a need to develop a dynamic drapability measurement method that utilizes reciprocating motion in order to simulate fabric drapability that is similar to that under practical conditions.

With the aim of overcoming the limitations of the existing drapability measurement methods, this study replicated the movement of fabrics under actual use conditions to propose a measurement method that applies reciprocating motion. As a method that properly reflects fabrics' actual drape characteristics through quantitative analysis using numbers, it is able to overcome the limitations present in existing test methods for static and dynamic drapability. Furthermore, through regression analysis that applies the physical properties of fabrics, such as bending and tensile behaviors, the factors that affect dynamic drapability were explored.

## Methods

### Samples

With reference to Sanad and Cassidy (2015), who demonstrated the impact of fabric weight on drapability, this study considered a total of 780 fabrics according to their drape coefficients and weights, and five representative samples (R1, R2, R3, R4, and R5) were used to develop the test method. Table 1(a) summarizes the properties of the five fabrics. Regarding the 780 fabrics, the average drape coefficient (%) was 32.51, with a minimum value of 2.65 and a maximum value of 97.92. The average weight ( $\text{g/m}^2$ ) was 183.27, with a minimum value of 19.49 and a maximum value of 420.6 (Kim et al., 2020). To determine the optimal conditions, four fabrics (R12, R23, R34, and R45) with median property values between each of the five representative samples were selected. Lastly, to verify the developed measurement method, four pairs of fabrics (A1 and A2, B1 and B2, C1 and C2, and D1 and D2) with similar drape coefficients but different drape shapes and weights were selected, as listed in Table 1(b). The drape shapes in Table 1(b) were obtained using ImageJ software (National Institute of Health, United States of America).

The fabric length was set as 50 cm or 100 cm, based on the average skirt length (50 cm to 57.5 cm) and the dress length (100.1 cm) per the International Size Reference Guide (Amanpreet & Saggi, 2014; Kocijančić, 2018). The width of the fabrics was set as 20 cm, considering the width of the affixing apparatus on the reciprocating motion device developed to measure the dynamic drapability. Given the circumstances of clothing production, the warp direction was aligned to the fabric length (50 cm or 100 cm), and the weft direction was aligned to the fabric width (20 cm). The physical properties in Table 1(a) were used to estimate the dynamic drapability through regression analysis. The bending property ( $M$ ; moving distance) was measured according to the warp and weft directions using a Cantilever stiffness tester, according to ISO 9073–7 (ISO, 1995). The tensile properties were measured in the warp, weft, and bias directions using a Universal Testing System (3344, Instron) per the ISO 9073–7 (ISO, 1995). Since the force that impacts drapability is markedly smaller than that used to examine the general tensile property, five points were measured until the point of nonlinear deformation of the curve was shown on the stress–strain graph. Here, the force (kgf) required for a 1% elongation is represented as  $F$ , and the second term coefficient of the stress–strain second-order function graph is represented as  $C$  (Kim et al., 2020).

### Characterization

#### *Measuring drapability using a device capable of reciprocating motion*









Figure 1a show the reciprocating motion device used in this study. To use the device, a fabric is fixed on the upper part of the device and made to move in reciprocating motion by adjusting the width and speed (rpm). The width can be adjusted from 50 to 200 mm, and the reciprocation speed (rpm) can be adjusted from 0 to 200.

After activating the reciprocating motion device, a digital camera (EOS M50 Mark2, Canon, Japan) was used to film the side of the hanging fabric for five seconds. TEMA Motion-Outer tracker (Image Systems Co., Ltd., Sweden) was utilized to analyze the outline of the fabric at a rate of 30 frames per second, to a total of 150 frames. When the outlines of 150 frames were accumulated, it became as shown in Fig. 1b. To translate the movement numerically, the center of the affixing apparatus is set as the origin (as

**Table 1** Physical, mechanical and drapery characteristics of fabric samples (a) Physical and mechanical characteristics (b) Drapery shapes of the test samples for verification

Sample code	Drape Coefficient (%)	Weight (g/m <sup>2</sup> )	Thickness (mm)	M <sub>WARP</sub>	M <sub>WEFT</sub>	F <sub>WARP</sub>	F <sub>WEFT</sub>	F <sub>BIAS</sub>	C <sub>WARP</sub>	C <sub>WEFT</sub>	C <sub>BIAS</sub>
<i>(a) Physical and mechanical characteristics</i>											
<i>Samples for measurement method development</i>											
R1	21.86	62.8	0.14	29	27	0.024	0.007	0.010	0.002	0.003	0.000
R2	34.70	158.4	0.30	31	29	0.010	0.010	0.010	0.001	0.000	0.000
R3	47.75	200.0	0.30	39	34	0.231	0.150	0.012	0.030	0.012	0.000
R4	78.43	232.3	0.33	44	71	0.020	0.099	0.022	-0.031	0.816	0.002
R5	94.73	305.1	0.46	54	37	0.596	0.219	0.133	0.020	-0.009	0.006
<i>Samples for identifying the optimal conditions</i>											
R12	26.66	102.0	0.25	39	33	0.011	0.001	0.010	0.000	0.231	0.000
R23	37.54	192.3	0.30	45	45	0.010	0.008	0.009	0.000	0.000	0.000
R34	52.68	207.0	0.36	41	47	0.009	0.010	0.008	0.024	0.002	0.000
R45	86.41	281.0	0.43	55	33	0.010	0.014	0.011	0.045	0.027	0.004
<i>Samples to verify the developed measurement method</i>											
A1	21.10	73.1	0.11	42	33	0.062	0.334	0.010	1.220	0.047	0.000
A2	26.31	209.0	0.44	29	26	0.010	0.010	0.010	0.000	0.000	0.000
B1	35.19	81.5	0.13	43	38	2.709	0.364	0.011	0.324	0.043	0.000
B2	30.20	292.0	0.64	35	31	0.010	0.011	0.009	0.000	0.001	0.000
C1	49.31	85.0	0.10	42	32	0.127	0.013	0.014	0.087	0.012	0.005
C2	48.53	169.1	0.31	32	49	0.030	0.256	0.010	0.010	0.080	0.000
D1	38.18	63.8	0.10	45	35	1.799	0.224	0.010	0.350	0.017	0.001
D2	37.88	305.0	1.15	35	29	0.011	0.009	0.010	0.000	0.000	0.000

**Table 1** (continued)

Sample code	Drape shape	Sample code	Drape shape	Sample code	Drape shape	Sample code	Drape shape
A1		B1		C1		D1	
A2		B2		C2		D2	

(b) Drape shapes of the test samples for verification

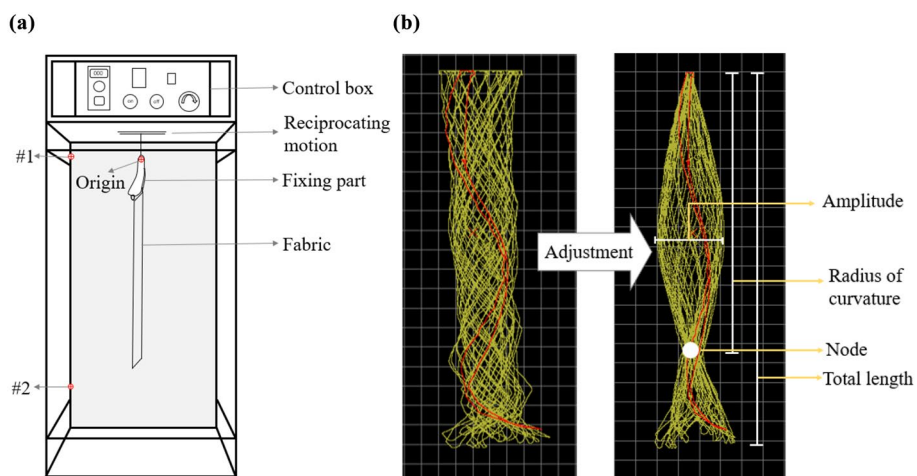


**Fig. 1** Drapability measuring device and an example of the analysis process; (a) drapability measuring device and (b) an example of fabric drapability analysis

shown in Fig. 1a), and the fabric movement shape is adjusted. An XY-coordinate system is determined using Points #1 and #2, for which the distance between the points is known. Based on analysis following the abovementioned procedure, the following significant factors were identified: node, node position, amplitude, total length, and movement area. A node refers to the protuberance created by the fabric movement, and it is determined by the most convex part in the image in which the moving shape of the reciprocating fabric is accumulated. The node position is the length from the top of fabric to the first node, and amplitude is the greatest width formed in the fabric movement shape. The total length refers to the total length of the movement shape. The movement area was calculated in ImageJ software.

Fabric type and length, motion width, and reciprocating speed were set as variables. Width and speed, where movement changes according to drapability, were observed in a preliminary experiment, based on which the reciprocation widths were set as 25 mm, 50 mm, 75 mm, and 100 mm, and the reciprocation speeds were 50 rpm, 100 rpm, 150 rpm, and 200 rpm. The conditions that displayed distinguishable outcomes with respect to drapability were observed. Then, fabrics with similar drape coefficients but different drape shapes were used to verify whether the proposed method improved on the limitations of existing drapability measurement.

**Drape coefficient**

Following ISO 9073-9:2008, the Cusick drape meter was used to calculate the drape coefficient by measuring the projected area of fabrics with a 15-cm radius, each placed on a supporting disk with a 9-cm radius. A distance of 80 cm distance was established between the drape meter and the camera lens when filming the fabric. ImageJ software (National Institute of Health, United States of America) was used for the image analysis and area calculation. The drape coefficient was determined using Eq. (1):

$$D(\%) = \frac{C - B}{A - B} \times 100 \quad (1)$$

A : Area of the specimen (cm<sup>2</sup>)

B : Area of the supporting disk (cm<sup>2</sup>)

C : Specimen projection area (cm<sup>2</sup>)

D : Drape coefficient (%)

### Regression analysis

The regression analysis was conducted using IBM SPSS Statistics to analyze the differences between the developed dynamic drapability measurement method and the drape coefficients and try to predict the dynamic drapability using the physical properties of the fabrics. The newly developed factors in this study and the drape coefficient were used as dependent variables, and the physical properties listed in Table 1 were used as independent variables.

## Results and Discussion

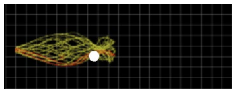
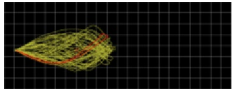
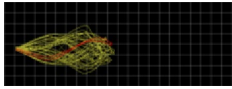
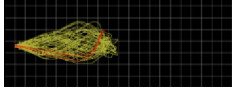
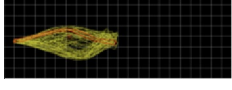
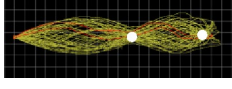
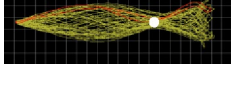
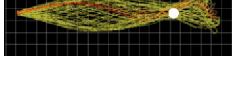
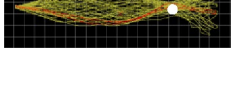
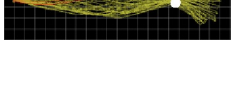
### The effects of fabric length on the dynamic fabric drapability

Various reciprocation widths and speeds were employed to examine the effect of fabric length (50 and 100 cm) on the dynamic drapability. Table 2 summarizes the shapes of five fabrics with respect to dynamic drapability under the condition of a 150-rpm reciprocation speed and a 75-mm width, which demonstrated the greatest difference due to fabric length. In the case of 100-cm fabrics, it was possible to more clearly observe node formation, and the nodes were more numerous, yielding a wider range of results than the 50-cm fabrics. Furthermore, the differences in node position and total length, which varied according to fabric drapability, were easier to observe in the 100-cm fabrics. In the process of transmitting force by the reciprocation motion to the fabric, longer fabrics produced relatively more curves, allowing for easy observation of movements. Based on the findings, the sample length was set at 100 cm in the following experiments that investigated the impacts of the reciprocation motion device's reciprocation speed and width.

### The effects of reciprocation width on the dynamic fabric drapability

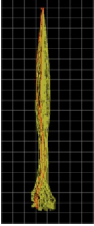
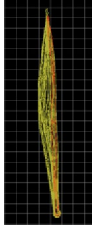
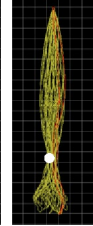
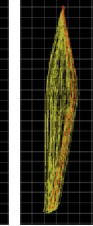
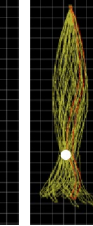
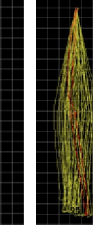
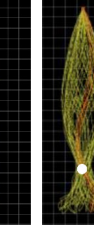
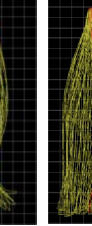
By varying the reciprocation speed under the reciprocation width conditions of 25, 50, 75, and 100 cm, it was verified whether the five types of fabrics differed in movement in terms of dynamic drapability. Table 3 and Additional file 1: Table S1 show the comparative results of the effects of reciprocation width at a 100-rpm reciprocation speed. With the 25-mm width, R1 and R5 did not form nodes, rendering it impossible to identify drapability through the fabrics' movement. For the 50-mm, 75-mm, and 100-mm reciprocation widths, nodes were formed in R1, which had more drapery and was lighter, rendering it possible to distinguish R1 from R5 through those nodes. Since motion due to greater reciprocation width applies greater force on fabrics, node formation is clearer in fabrics with more drapery, enabling distinctions between different types of fabrics. Even at reciprocation speeds other than 100 rpm, it was confirmed that greater reciprocation widths create greater movement amplitudes in fabrics, resulting in more nodes

**Table 2** Analytical results for dynamic drapability according to fabric length (movement width: 75 mm, reciprocation speed: 150 rpm)

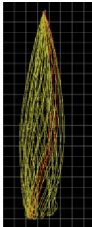
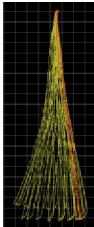
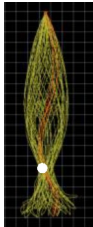
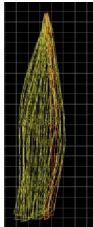
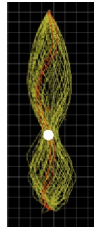
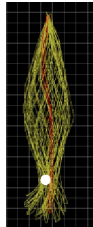
Sample	50					100				
	R1	R2	R3	R4	R5	R1	R2	R3	R4	R5
Analysis image										
Number of nodes	1	0	0	0	0	2	1	1	1	1
Node position (cm)	39.01	-	-	-	-	57.33/91.39	67.73	73.26	74.19	76.68
Amplitude (cm)	15.90	19.08	22.92	18.24	16.57	16.90/16.73	16.64	15.23	17.14	16.81
Total length (cm)	48.72	49.08	47.62	49.63	50.00	95.85	96.04	98.32	98.62	100.00
Area (cm <sup>2</sup> )	583.31	703.70	697.86	655.36	572.30	1349.62	1181.52	1275.84	1339.68	1277.76



**Table 3** Analytical results for dynamic drapability according to reciprocation width (speed: 100 rpm)

Reciprocation width (mm)	25		50		75		100	
	R1	R5	R1	R5	R1	R5	R1	R5
Analysis image								
Number of nodes	0	0	1	0	1	0	1	0
Node position (cm)	–	–	71.80	–	70.50	–	76.19	–
Amplitude (cm)	6.72	8.37	11.26	14.28	15.80	17.07	19.75	20.01
Total length (cm)	98.89	100.00	99.74	100.00	96.04	100.00	99.45	100.00
Area (cm <sup>2</sup> )	798.43	770.86	927.12	1518.05	1330.70	1524.03	1580.60	1722.08

**Table 4** Analytical results for dynamic drapability according to reciprocation speed (width: 100 mm)

RPM	50		100		150	
	R1	R5	R1	R5	R1	R5
Analysis image						
Number of nodes	0	0	1	0	1	1
Node position (cm)	–	–	76.19	–	58.61	78.46
Amplitude (cm)	19.92	–	19.75	20.01	19.38	22.02
Total length (cm)	100.00	100.00	99.45	100.00	95.97	99.93
Area (cm <sup>2</sup> )	2155.22	2054.64	1580.60	1722.08	1540.82	1590.55

and higher node location. Therefore, under identical reciprocation speed conditions, it was deemed that dynamic drapability may be observed through various factors when the reciprocation width is large.

**The effects of reciprocation speed on the dynamic fabric drapability**

To observe the effect of the reciprocation speed, the fabric drapability was observed under the speed conditions of 50 rpm, 100 rpm, 150 rpm, and 200 rpm. Considering the potential malfunction of the developed device when made to produce wide movements at various reciprocation speeds, observations were not made for the

75-mm and 100-mm under the 200-rpm condition. As shown in Table 4 and Additional file 1: Table S2, under the condition of a 50-rpm speed and a 100-mm width, the fabrics' movements were not sufficiently significant to display differences. However, under the conditions of 100 rpm and 150 rpm, distinct curves formed depending on the fabrics. This result demonstrates that under a constant width condition, as shown in Eq. 2, a faster reciprocation speed produces a higher frequency ( $\omega$ ), increasing acceleration ( $a$ ). In turn, as shown in Eq. 3, it delivers greater force ( $F$ ) to the fabric, thus shortening the radius of the curvature (Yu et al., 2021). This outcome was replicated in other width conditions, where, under a constant rpm, smaller widths were found to apply less force to the fabrics, thus creating simpler fabric movements.

$$a = \frac{d^2x}{dt^2} = -\omega^2 A \cos(\omega t + \varnothing) \quad (2)$$

$x$ : Displacement in the direction of vibration.

$A$ : Amplitude.

$\omega$ : Frequency

$$F = ma = kx \quad (3)$$

$m$ : Mass of the object

$a$ : Acceleration

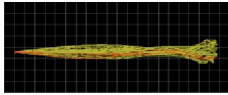
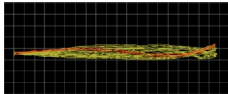
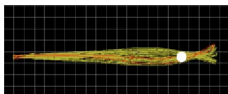
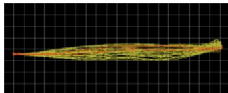
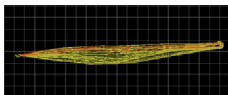
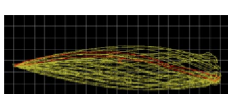
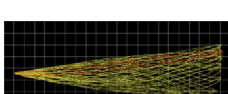
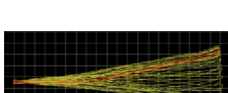
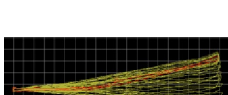
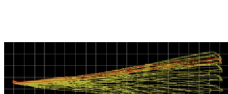
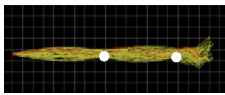
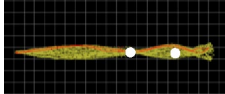
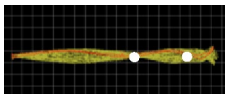
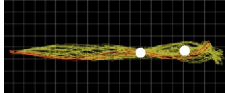
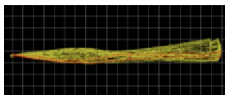
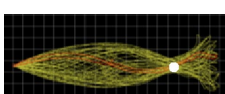
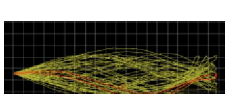
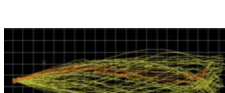
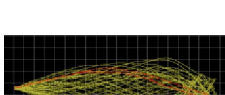
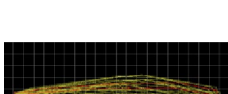
$k$ : Spring constant

$x$ : Displacement from the equilibrium position

### Analysis of the condition of exerting a constant force

Favorable conditions for measuring drapability were investigated under the condition of exerting a constant force with varying reciprocation widths and speeds. As shown in Eqs. (2) and (3), reciprocation width corresponds to amplitude ( $A$ ), which is proportional to acceleration ( $a$ ) and force ( $F$ ), and reciprocation speed corresponds to frequency ( $\omega$ ), which is proportional to the square of acceleration ( $a$ ) and force ( $F$ ). The conditions displayed in Table 5 were set based on the aforementioned equations. As indicated in Table 5(a), despite the difficulty of demonstrating drapability for both conditions, the condition of a 25-mm width and a 100-rpm speed created curves in the fabrics, forming nodes and different drape shapes for each fabric. However, under the condition of a 100-mm width and a 50-rpm speed, the fabrics produced similar drape shapes because of the low speed, rendering it unfeasible to measure drapability. As shown in Table 5(b), the condition of a 25-mm width and a 200-rpm speed created curves in the fabrics, forming distinct movement shapes. Compared with the conditions shown in Table 5(a), those in Table 5(b) theoretically produced a force that was four times greater. Nevertheless, under the condition of a 100-mm width and a 100-rpm speed, there were far fewer curves in the fabrics, and their movements were not sufficient to measure drapability. These findings suggest that fabric movements are more diverse with greater force and that, under a constant force, a narrower reciprocation width and a faster reciprocation

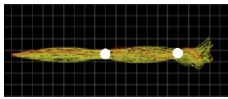
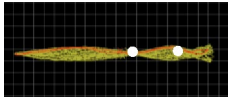
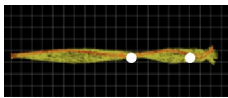
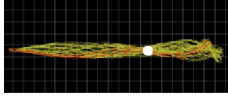
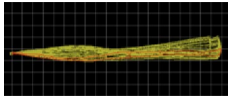
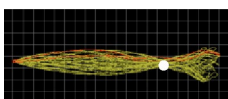
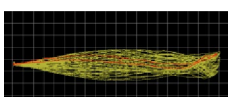
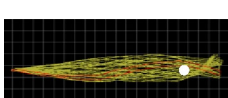
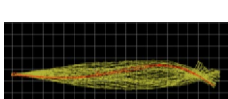
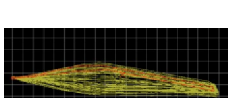
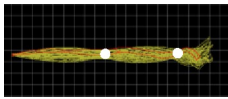
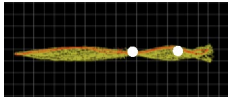
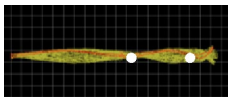
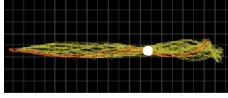
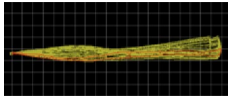
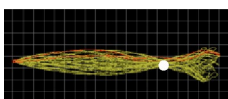
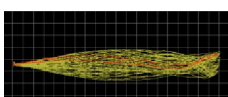
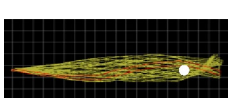
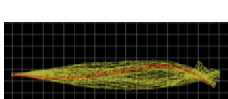
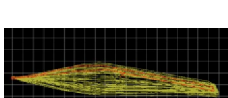
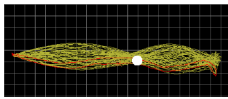
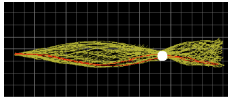
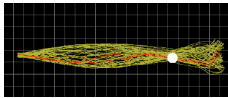
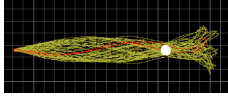
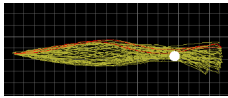
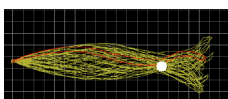
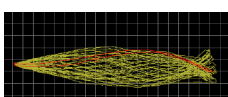
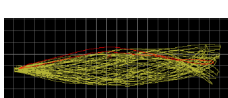
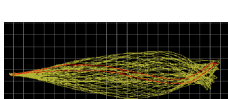
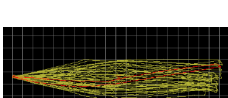
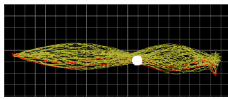
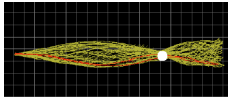
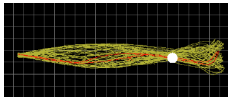
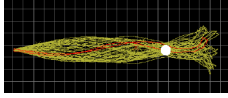
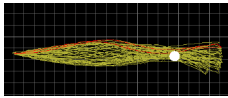
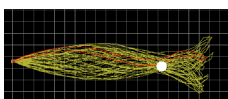
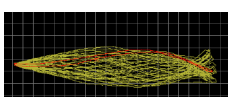
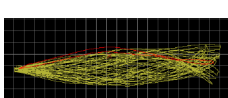
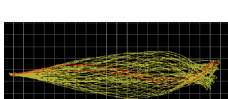
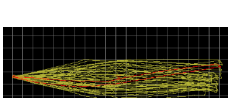
**Table 5** Analytical results for dynamic drapability under a constant force

Condition	25 mm, 100 rpm					100 mm, 50 rpm				
	R1	R2	R3	R4	R5	R1	R2	R3	R4	R5
<i>(a) Reciprocation of 25 mm width and 100 rpm speed vs. reciprocation of 100 mm with and 50 rpm speed</i>										
Analysis image										
Number of nodes	0	0	1	0	0	0	0	0	0	0
Node position (cm)	-	-	87.36	-	-	-	-	-	-	-
Amplitude (cm)	6.72	7.54	8.20	8.05	8.37	19.92	-	-	-	-
Total length (cm)	98.89	99.09	98.35	100.00	100.00	100.00	100.00	100.00	100.00	100.00
Area (cm <sup>2</sup> )	798.43	770.86	798.76	896.41	875.65	2155.22	2078.98	1861.61	1945.63	2054.64
<b>Condition</b>										
<b>25 mm, 200 rpm</b>										
<b>Sample</b>	<b>R1</b>	<b>R2</b>	<b>R3</b>	<b>R4</b>	<b>R5</b>	<b>R1</b>	<b>R2</b>	<b>R3</b>	<b>R4</b>	<b>R5</b>
<i>(b) Reciprocation of 25 mm width and 200 rpm speed vs. reciprocation of 100 mm with and 100 rpm speed</i>										
Analysis image										

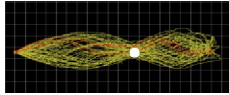
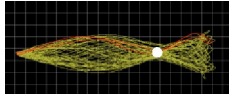
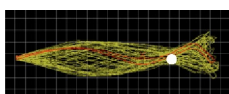
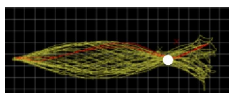
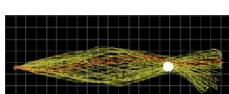
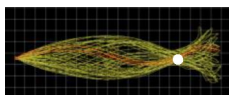
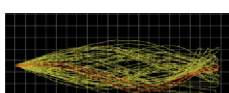
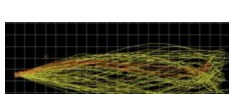
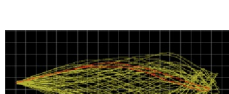
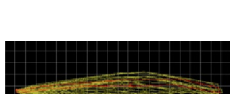
**Table 5** (continued)

Condition	25 mm, 200 rpm					100 mm, 100 rpm				
	R1	R2	R3	R4	R5	R1	R2	R3	R4	R5
Number of nodes	2	2	2	2	0	1	0	0	0	0
Node position (cm)	42.49/76.74	57.36/86.79	58.79/92.68	57.36/86.79	-	76.19	-	-	-	-
Amplitude (cm)	6.53/7.70	6.05/7.06	6.2/6.52	6.05/7.06	-	19.75	23.70	21.36	25.10	20.01
Total length (cm)	96.34	96.97	97.80	96.97	99.82	99.45	99.36	100.00	99.57	100.00
Area (cm <sup>2</sup> )	596.38	509.12	497.57	509.12	673.05	1580.60	2064.37	2016.57	1686.79	1722.08

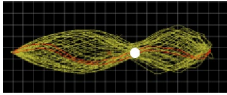
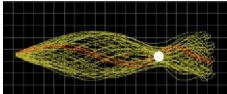
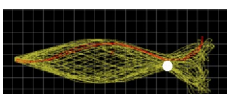
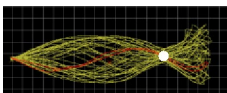
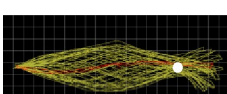
**Table 6** Analytical results for dynamic drapability per fabric condition

Condition	25 mm, 200 rpm					50 mm, 100 rpm				
	R1	R2	R3	R4	R5	R1	R2	R3	R4	R5
Sample										
Analysis image										
Number of nodes	2	2	2	1	0	1	0	1	0	0
Node position (cm)	42.49/76.74	57.36/86.79	58.79/92.68	60.62	-	71.80	-	91.41	-	-
Amplitude (cm)	6.53/ 7.70	6.05/ 7.06	6.2/ 6.52	6.87	-	11.26	13.22	11.93	13.06	14.28
Total length (cm)	96.34	96.97	97.80	99.45	99.82	99.74	99.93	100.00	100.00	100.00
Area (cm <sup>2</sup> )	596.38	509.12	497.57	558.84	673.05	927.12	1337.75	1441.05	1293.16	1518.05
Condition	50 mm, 150 rpm					75 mm, 100 rpm				
Sample										
Analysis image										
Number of nodes	1	1	1	1	1	1	1	0	0	0
Node position (cm)	55.13	69.21	71.61	73.26	75.64	70.50	87.01	-	-	-

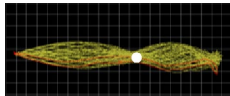
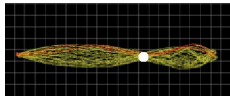
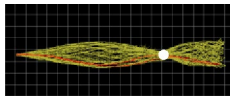
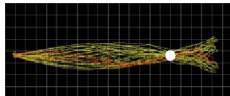
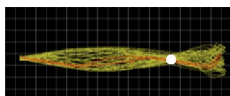
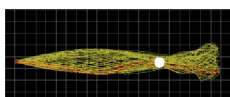
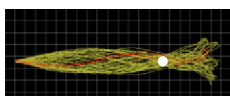
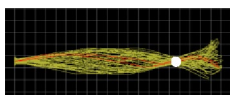
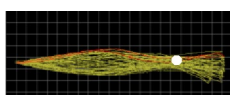
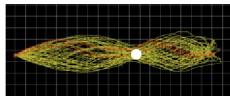
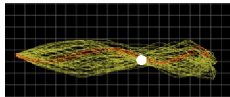
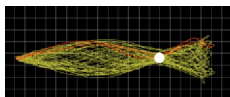
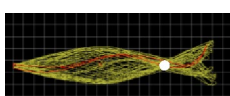
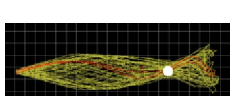
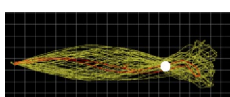
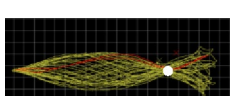
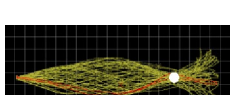
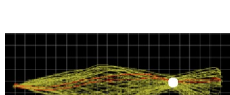
**Table 6** (continued)

Condition	50 mm, 150 rpm					75 mm, 100 rpm				
	R1	R2	R3	R4	R5	R1	R2	R3	R4	R5
Amplitude (cm)	12.39	11.26	10.54	11.25	11.55	15.80	16.64	16.47	20.92	17.07
Total length (cm)	99.27	99.56	99.45	99.27	100.00	96.04	97.51	98.63	100.00	100.00
Area (cm <sup>2</sup> )	1001.23	894.08	939.96	939.64	946.37	1330.70	1324.92	1500.72	1317.54	1524.03
Condition	75 mm, 150 rpm					100 mm, 100 rpm				
Sample	R1	R2	R3	R4	R5	R1	R2	R3	R4	R5
Analysis image										
Number of nodes	2	1	1	1	1	1	0	0	0	0
Node position (cm)	57.33/91.39	67.73	73.26	73.99	76.68	76.19	-	-	-	-
Amplitude (cm)	16.90/16.73	16.64	15.23	16.73	16.81	19.75	23.70	21.36	25.10	20.01
Total length (cm)	95.85	96.04	98.32	98.71	100.00	99.45	99.36	100.00	99.57	100.00
Area (cm <sup>2</sup> )	1349.62	1181.52	1275.84	1339.68	1277.76	1580.60	2064.37	2016.57	1686.79	1722.08

**Table 6** (continued)

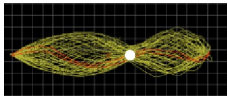
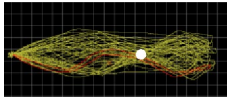
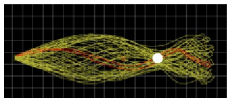
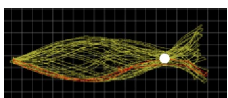
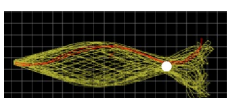
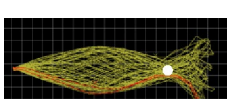
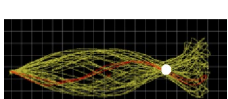
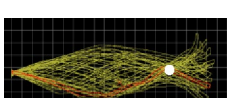
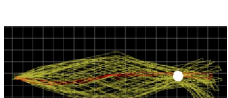
Condition		100 mm, 150 rpm				
Sample		R1	R2	R3	R4	R5
Analysis image						
Number of nodes		1	1	1	1	1
Node position (cm)		58.61	69.21	72.34	73.99	78.46
Amplitude (cm)		19.38	20.84	19.75	20.08	22.02
Total length (cm)		95.97	96.97	97.07	97.44	99.93
Area (cm <sup>2</sup> )		1540.82	1590.23	1505.85	1756.40	1590.55

**Table 7** Analytical results for identifying the optimal condition for measuring dynamic drapability

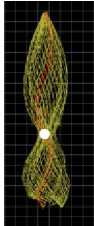
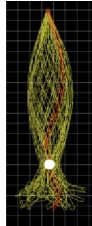
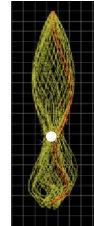
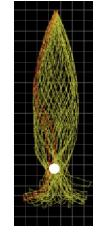
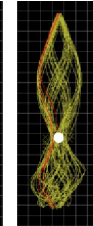
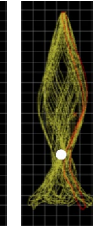
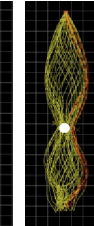
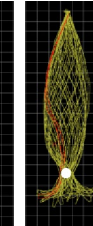
Condition		50 mm, 150 rpm									
Sample		R1	R12	R2	R23	R3	R34	R4	R45	R5	
Analysis image											
Number of nodes	1	1	1	1	1	1	1	1	1	1	1
Node position (cm)	55.13	60.62	74.36	71.61	72.72	73.26	77.02	75.64			
Amplitude (cm)	12.39	10.21	11.55	10.54	11.05	11.25	10.67	11.55			
Total length (cm)	99.27	97.62	99.09	99.45	99.27	99.27	100.00	100.00			
Area (cm <sup>2</sup> )	1001.23	762.09	917.60	939.96	945.28	939.64	917.59	946.37			
Condition		75 mm, 150 rpm									
Sample		R1	R12	R2	R23	R3	R34	R4	R45	R5	
Analysis image											
Number of nodes	2	1	1	1	1	1	1	1	1	1	1
Node position (cm)	57.33/91.39	61.35	67.73	71.61	73.26	73.99	74.19	76.68			
Amplitude (cm)	16.90/16.73	16.40	16.64	16.07	15.23	16.73	17.14	16.81			



**Table 7** (continued)

Condition		75 mm, 150 rpm									
Sample	R1	R12	R2	R23	R3	R34	R4	R45	R5		
Total length (cm)	95.85	97.44	96.04	97.25	98.32	98.72	98.71	98.62	100.00		
Area (cm <sup>2</sup> )	1349.62	1284.62	1181.52	1103.21	1275.84	1484.18	1339.68	1362.63	1277.76		
Condition		100 mm, 150 rpm									
Sample	R1	R12	R2	R23	R3	R34	R4	R45	R5		
Analysis image											
Number of nodes	1	1	1	1	1	1	1	1	1		
Node position (cm)	58.61	60.62	69.21	71.98	72.34	72.98	73.99	75.87	78.46		
Amplitude (cm)	19.38	19.67	20.84	19.58	19.75	20.25	20.08	22.48	22.02		
Total length (cm)	95.97	96.80	96.97	94.87	97.07	96.34	97.44	98.63	99.93		

**Table 8** Analytical results on dynamic drapability for samples (width: 100 mm; reciprocation speed: 150 rpm)

Sample	A1	A2	B1	B2	C1	C2	D1	D2
Analysis image								
Number of nodes	1	1	1	1	1	1	1	1
Node position (cm)	59.21	75.50	59.95	77.17	60.85	69.39	56.04	78.46
Amplitude (cm)	20.34	19.33	18.66	19.50	19.33	20.84	18.83	19.33
Total length (cm)	94.14	97.34	96.41	96.23	94.99	96.23	97.70	95.12
Area (cm <sup>2</sup> )	1378.62	1442.31	1373.37	1541.26	1412.11	1380.15	1309.24	1344.04

speed will produce significant movements that can be quantified, creating distinctions between different fabrics.

According to the above results for the five types of fabrics with a length of 100 cm, a total of seven conditions among the 13 conditions with varying reciprocation widths (25, 50, 75, and 100 mm) and speeds (50, 100, 150, and 200 rpm) could significantly measure fabrics' dynamic drapability based on the fabric movement. The seven plausible conditions are 25 mm, 200 rpm; 50 mm, 100 rpm; 50 mm, 150 rpm; 75 mm, 100 rpm; 75 mm, 150 rpm; 100 mm, 100 rpm; and 100 mm, 150 rpm.

**Analysis of the movement per condition and selection of measurement factors**

Table 6 summarizes the movement analysis results under the seven aforementioned conditions. Under the condition of a 25-mm reciprocation width and a 200-rpm speed, R5 did not form nodes, rendering the condition unsuitable to quantify drape characteristics. Furthermore, for the three width conditions moving at 100 rpm, there were no sequential changes in discrimination factors such as node position or total length, and thus, these conditions were excluded from the group of significant conditions for measuring dynamic drapability. Therefore, among the seven selected conditions, the following conditions that showed sequential changes in node position according to fabric type were deemed suitable for measuring dynamic drapability: a reciprocation of a 50-mm width at a speed of 150 rpm, a 75-mm width at a speed of 150 rpm, and a 100-mm width at a speed of 150 rpm.

Based on the outcomes for the seven selected conditions, the factors that best described the dynamic drapability were selected from the original five factors (i.e., the number of nodes, the position of the first node, amplitude, total length, and surface area) to replace the existing drape coefficient. In respect to the number of nodes, the number tended to increase

**Table 9** Regression analysis on the drape coefficient and the node position (a) Dependent variable: Drape coefficient (%) (b) Dependent variable: Node position

Independent variables	Unstandardized coefficients		Standardized coefficients $\beta$	t(p)	Significance*
	B	Standard error			
<i>(a) Dependent variable: drape coefficient (%)</i>					
(Constant)	- 48.024	13.158		- 3.650	0.003
$M_{WARP}$	2.338	0.331	0.815	7.053	0.001
$C_{WARP}$	- 51.121	10.967	- 0.704	- 4.661	0.001
$F_{WARP}$	- 13.786	4.483	- 0.472	- 3.075	0.010
$F_{WEFT}$	102.805	33.095	0.598	3.106	0.009
Adjusted R <sup>2</sup>	0.805				
Equation	$y = -48.024 + 2.338M_{WARP} - 51.121C_{WARP} - 13.786F_{WARP} + 102.805F_{WEFT}$				
<i>(b) Dependent variable: Node position</i>					
(Constant)	61.678	2.620		23.544	0.000
Weight	0.092	0.007	0.965	13.609	0.000
$M_{WARP}$	- 0.217	0.064	- 0.241	- 3.402	0.004
Adjusted R <sup>2</sup>	0.911				
Equation	$y = 61.678 + 0.092Weight - 0.217M_{WARP}$				

\*Statistically significant at  $p < 0.05$

in drapery fabrics, but since too few nodes were formed, the factor was deemed unsuitable for distinguishing between various fabrics. Regarding the position of the first node, under the condition of a 50-mm reciprocation width and a speed of 150 rpm, the R1 fabric formed the highest-positioned node at 55.13 cm, whereas R5, the stiffest and heaviest fabric, formed the lowest-positioned node at 75.64 cm. This trend was replicated in other conditions, namely a 75-mm reciprocation width and a speed of 150 rpm and a 100-mm width and a speed of 150 rpm, demonstrating that the factor “first node position” reflects dynamic drapability well. Regarding amplitude, as shown under the condition of a 75-mm reciprocation width and a 100-rpm speed, a trend was apparent up to sample R4, but no sequential result occurred in R5. Similarly, for the condition of a 100-mm reciprocation width and a 100-rpm speed, a trend appeared, excluding R1 and R3. Hence, the amplitude factor was deemed inaccurate in terms of determining dynamic drapability. In respect to the total length, under most conditions, the length progressively increased from R1 to R5, but there were conditions where distinctions were not apparent between R2, R3, and R4. Lastly, when comparing the fabrics’ movement area across the conditions, no evident trends in relation to drapability were observed. Based on these results, the position of the first node was identified as the factor that is the most significant in measuring dynamic drapability.

**Confirmation of the optimal condition for measuring dynamic drapability**

It was aimed to confirm the optimal condition, among abovementioned three conditions, based on movement analysis according to the position of the first node. Four types of fabrics (R12, R23, R34, R45) with median characteristics between each of the five samples used to identify the three conditions were selected. Hence, a total of nine fabric samples were used to determine the optimal condition for measuring dynamic drapability.

As shown in Table 7, under the condition of a 50-mm reciprocation width and a speed of 150 rpm, R2's first-node position was 69.21 cm and R3's was 71.61 cm. For their middle sample, R23, the node position was 74.36 cm, contradicting the prediction that the node position would lower sequentially. Furthermore, under the condition of a 75-mm reciprocation width and a speed of 150 rpm, fabric sample R34, the middle sample between R3 and R4, formed a node at 71.80 cm, which was not between the R3 and R4 node positions of 73.26 cm and 73.99 cm, respectively, demonstrating the unsuitability of the condition for measuring dynamic drapability. Lastly, under the condition of a 100-mm reciprocation width and a speed of 150 rpm, each type of fabric formed nodes at a lower position in sequence, indicating that this is the optimal condition to measure dynamic drapability. As previously described in the analysis of force, given a constant reciprocation speed (150 rpm), a greater reciprocation width delivers more force to the fabric, which, in turn, best defines dynamic drapability according to the movement of the fabric.

#### **Verification the test method developed for a dynamic drapability**

One of the limitations of the existing drapability measurement methods is that the drape coefficient based on the area cannot distinguish between differences in drapability given variance in drape shape, despite similar area size. Hence, this study sought to verify whether the developed dynamic drapability measurement method could overcome such a shortcoming through four pairs of samples indicated in Table 1. Table 8 summarizes the results of the analysis. When comparing the drapability of fabrics using the position of the first node, which was found to be the most significant factor for examining dynamic drapability, it was noted that the relatively heavier fabrics, namely A2, B2, C2, and D2, formed their first nodes higher on the fabric than their lighter counterparts. As previously mentioned, more force is required for identical reciprocation motion with heavier fabrics, which delivers more force to the fabric and shortens the radius of the curvature, a principle that is reflected in the position of the first node. This finding confirms that the developed drapability measurement method is capable of distinguishing between fabrics with similar drape coefficients but different drape properties. Therefore, it was deemed that fabric weight influences node position, which represents the dynamic drapability.

#### **Prediction of the dynamic drapability based on physical properties**

Regression analysis with the physical properties of fabrics as independent variables was conducted to compare the developed dynamic drapability measurement method and the existing drapability coefficient and examine the factors that influence the differences between the two. As shown in Table 9(a), the factors that had significant influence on the drape coefficient ( $p < 0.05$ ) were properties related to tensile and bending behaviors, namely  $M_{\text{WARP}}$ ,  $C_{\text{WARP}}$ ,  $F_{\text{WARP}}$ , and  $F_{\text{WEFT}}$ , and the explanatory power (adjusted  $R^2$ ) of the regression equation was 80.5%. Since this model does not include the weight of the fabric, a physical property that is known to be significant to measuring drapability, it cannot distinguish between fabrics with similar drape coefficients but different shapes.

An advantage of this method, however, is that the direction of the fabric does not need to be considered when measuring drapability since the warp, weft, and bias directions exert equal influence due to the circular shape of the fabric used during measurement. As shown in Table 9(b), the regression analysis where the node position of the developed measurement method was the dependent variable and the weight and bending property of  $M_{\text{WARP}}$  were independent variables had an explanatory power (adjusted  $R^2$ ) of 91.1%. As evidenced in the measurement method development process, dynamic drapability is largely influenced by weight and bending properties ( $p < 0.05$ ). However, this method was formulated using only fabrics' warp direction and thus may have less significance in relation to other directions such as weft and bias.

## Conclusions

This study aimed to develop a method that measures dynamic drapability via reciprocating motion by imitating the shape of movements created during the actual use of fabrics. Five fabrics were selected for measurement based on their drape coefficients and weights, and the lengths of fabrics were set as 50 cm and 100 cm. By controlling the width and speed of reciprocation, the fabrics' drapability was observed under various conditions. It was found that all conditions at lower speeds lacked distinguishability and that there were distinguishable movements at medium and high speeds with narrower reciprocation widths. This outcome indicates the impact of the force delivered to the fabric, where a higher speed generates a greater force, causing the fabric to form more various movements, ultimately producing distinguishability between different fabrics. The position of the first node created during these reciprocating movements demonstrated the most similar outcomes with respect to the fabrics' dynamic drapability. Four additional samples with median characteristics between each of the five samples were used to identify the optimal condition. Results of nine fabric samples and the position of their first nodes indicate that a reciprocation width of 100 mm and a speed of 150 rpm constitute the optimal condition to achieve distinguishable drapability. Furthermore, four pairs of fabrics with similar drape coefficients but different drape shapes were included to verify whether the developed measurement method could identify differences within each pair. It was confirmed that the positions of the first node in each pair could differentiate between the two fabrics. Regression analysis showed that the weight and bending properties of warp direction of fabrics have the greatest impacts on the position of the first node.

This study is basic research on the development of a method to measure dynamic drapability through reciprocating motion. In order for this study to be more meaningful, it is thought that further research is needed to examine the correlation between reciprocating motion and dynamic drapability of fabrics. Moreover, this study set the warp direction, which is the commonly used direction of fabrics, in the length direction, but additional research that considers the warp and bias directions is necessary as well.

## Supplementary Information

The online version contains supplementary material available at <https://doi.org/10.1186/s40691-023-00355-7>.

**Additional file 1: Table S1.** Analytical results for dynamic drapability according to reciprocation width (speed: 100 rpm). **Table S2.** Analytical results for dynamic drapability according to reciprocation speed (width: 100 mm).

### Acknowledgements

Not applicable.

### Authors' contributions

EY conceived the ideas, experimental design, performed the experiments, collected the data, interpretation of the results, and drafted the manuscript of the analysis. CY supervised on the experimental design, experimental results, and manuscript preparation. All authors read and approved the final manuscript.

### Authors' information

EY received a Master degree from the Department of Fashion Industry at Ewha Womans University in 2023. She currently works at the Korea textile trade association. CY is an Associate Professor in the Department of Fashion Industry at Ewha Womans University. He received a Ph.D. from Seoul National University. His research group is to explore the textile-based science & technology for sustainable fashion.

### Funding

This paper was conducted with the support of the Industrial Technology Innovation Infrastructure Project of Korea Institute for Advancement of Technology in 2022 (No. P0014711).

## Declarations

### Competing interests

The authors declare that they do not have any competing interests.

Received: 8 March 2023 Accepted: 6 August 2023

Published online: 25 September 2023

## References

- Amanpreet, K., & Saggi, H. K. (2014). Preferences of college girls for fabrics, colours, designs, length, flare and other designing features in one piece dresses. *Asian Journal of Home Science*, 9(2), 576–579. <https://doi.org/10.15740/HAS/AJHS/9.2/576-579>
- American Society for Testing and Materials. (2018). *Standard test method for stiffness of fabrics* (ASTM Standard No. D 1388–18). <https://www.astm.org/d1388-18.html>
- British Standard. (1973). *Method for the assessment of drape of fabrics* (BS Standard No. 5058). <https://standards.globalspec.com/std/167368/BS%205058>
- Collier, B. J., Paulins, V. A., & Collier, J. R. (1989). Effects of interfacing type on shear and drape behavior of apparel fabrics. *Clothing and Textiles Research Journal*, 7(3), 51–56. <https://doi.org/10.1177/0887302X89007003>
- Collier, J. R., Collier, B. J., O'Toole, G., & Sargand, S. M. (1991). Drape prediction by means of finite-element analysis. *Journal of the Textile Institute*, 82(1), 96–107. <https://doi.org/10.1080/00405009108658741>
- Cusick, G. E. (1965). 46—The dependence of fabric drape on bending and shear stiffness. *Journal of the Textile Institute Transactions*, 56(11), T596–T606. <https://doi.org/10.1080/19447026508662319>
- International Organization for Standardization. (1995). *Textiles—Test methods for nonwovens—Part 7: Determination of bending length* (ISO Standard No. 9073-7:1995). <https://www.iso.org/standard/16657.html>
- Ji, F., Li, R., & Qiu, Y. (2006). Simulate the dynamic draping behavior of woven and knitted fabrics. *Journal of Industrial Textiles*, 35(3), 201–215. <https://doi.org/10.1177/1528083706055753>
- Kenkare, N., & May-Plumlee, T. (2005). Evaluation of drape characteristics in fabrics. *International Journal of Clothing Science and Technology*, 17(2), 109–123. <https://doi.org/10.1108/09556220510581254>
- Kilic, G. B., Demir, M., & Kilic, M. (2021). Dynamic drape behaviours of wool woven suiting fabrics considering real-time use. *International Journal of Clothing Science and Technology*, 33(5), 811–823. <https://doi.org/10.1108/IJCT-11-2020-0173>
- Kim, J., Kim, Y. J., Shim, M., Jun, Y., & Yun, C. (2020). Prediction and categorization of fabric drapability for 3D garment virtualization. *International Journal of Clothing Science and Technology*, 32(4), 523–535. <https://doi.org/10.1108/IJCT-08-2019-0126>
- Kocijančić, Đ. (2018). Research and investigation of women's dress pattern. *Textile & Leather Review*, 1(3–4), 100–113. <https://doi.org/10.31881/TLR.2018.vol1.iss3-4.p100-113.a10>
- Lim, H. S. (2009). *Three dimensional virtual try-on technologies in the achievement and testing of fit for mass customization* [Doctoral dissertation, North Carolina State University]. NCSU Repository. <http://www.lib.ncsu.edu/resolver/1840.16/3322>
- Matsudaira, M., Yang, M., Kinari, T., & Shintaku, S. (2002). Polyester "Shingosen" fabrics characterized by dynamic drape coefficient with swinging motion. *Textile Research Journal*, 72(5), 410–416. <https://doi.org/10.1177/004051750207200507>

- Morooka, H., & Niwa, M. (1976). Relation between drape coefficients and physical properties of fabrics. *Journal of the Textile Machinery Society of Japan*, 22(3), 67–73. <https://doi.org/10.4188/jte1955.22.67>
- Sanad, R., & Cassidy, T. (2015). Investigating garment drape behaviour. *Journal of Fiber Bioengineering and Informatics*, 8(1), 47–56. <https://doi.org/10.3993/jfbi03201505>
- Sarakatsanos, O., Chatzilari, E., Nikolopoulos, S., Kompatsiaris, I., Shin, D., Gavilan, D., & Downing, J. (2021). A VR application for the virtual fitting of fashion garments on avatars. *2021 IEEE International Symposium on Mixed and Augmented Reality Adjunct (ISMAR-Adjunct)*, Italy, 40–45. <https://doi.org/10.1109/ISMAR-Adjunct54149.2021.00018>
- Süle, G. (2012). Investigation of bending and drape properties of woven fabrics and the effects of fabric constructional parameters and warp tension on these properties. *Textile Research Journal*, 82(8), 810–819. <https://doi.org/10.1177/0040517511433152>
- Wang, P. N., & Cheng, K. B. (2011). Dynamic drape property evaluation of natural fiber woven fabrics using a novel automatic drape-measuring system. *Textile Research Journal*, 81(13), 1405–1415. <https://doi.org/10.1177/0040517511404592>
- Yu, D., Yoon, J., Lee, S. W., & Yun, C. (2021). Improvement of dust removal performance through analysis on the physical behavior of fabric in the clothing care system. *Current Applied Physics*, 27, 117–124. <https://doi.org/10.1016/j.cap.2021.03.010>

### Publisher's Note

Springer Nature remains neutral with regard to jurisdictional claims in published maps and institutional affiliations.

**Eunbi Yun** received a Master degree from the Department of Fashion Industry at Ewha Womans University in 2023. She currently works at the Korea textile trade association.

**Changsang Yun** is an Associate Professor in the Department of Fashion Industry at Ewha Womans University. He received a Ph.D. from Seoul National University. His research group is to explore the textile-based science & technology for sustainable fashion.

Submit your manuscript to a SpringerOpen<sup>®</sup> journal and benefit from:

- ▶ Convenient online submission
- ▶ Rigorous peer review
- ▶ Open access: articles freely available online
- ▶ High visibility within the field
- ▶ Retaining the copyright to your article

---

Submit your next manuscript at ▶ [springeropen.com](https://www.springeropen.com)

---